JACS ARTICLES

Published on Web 12/13/2010

$LiCoO_2$ Concaved Cuboctahedrons from Symmetry-Controlled Topological Reactions

Hailong Chen,[†] Lijun Wu,[‡] Lihua Zhang,[‡] Yimei Zhu,[‡] and Clare P. Grey*[,†,§]

Department of Chemistry, Stony Brook University, Stony Brook, New York 11794-3400, United States of America; Brookhaven National Laboratory, Upton, New York 11973, United States of America; and Department of Chemistry, Cambridge University, Lensfield Rd, Cambridge, CB2 1EW, United Kingdom

Received June 15, 2010; E-mail: cpg27@cam.ac.uk

Abstract: Morphology control of functional materials is generally performed by controlling the growth rates on selected orientations or faces. Here, we control particle morphology by "crystal templating": by choosing appropriate precursor crystals and reaction conditions, we demonstrate that a material with rhombohedral symmetry—namely the layered, positive electrode material, $LiCoO_2$—can grow to form a quadruple-twinned crystal with overall cubic symmetry. The twinned crystals show an unusual, concaved-cuboctahedron morphology, with uniform particle sizes of 0.5−2 μm. On the basis of a range of synthetic and analytical experiments, including solid-state NMR, X-ray powder diffraction analysis and HRTEM, we propose that these twinned crystals form via selective dissolution and an ion-exchange reaction accompanied by oxidation of a parent crystal of CoO, a material with cubic symmetry. This template crystal serves to nucleate the growth of four $LiCoO_2$ twin crystals and to convert a highly anisotropic, layered material into a pseudo-3-dimensional, isotropic material.

Introduction

Many highly orientated thin films, or single crystals, show anisotropic chemical and physical properties, such as electronic and ionic conductivities, due to the intrinsic anisotropy of the crystal lattice. For example, in the field of lithium ion batteries (LIBs), Li ion diffusivity in both positive and negative electrodes, are often anisotropic, the conduction direction(s) being determined by the lowest activation barriers for Li migration. One-dimensional Li ion diffusion occurs in the electrode material $LiFePO_4$,[1,2] while in the commercial electrode material, $LiCoO_2$, the diffusion is 2-D. In principle, isotropic diffusion is desirable, since this results in a larger active surface area for Li-transfer from the electrolyte, potentially leading to improved LIB rate performance. Although it is very difficult to control the dimensionality of the conduction process, which is mostly determined by the lattice, control of the morphology and the assembly of the primary particles represent possible routes to alter the rate performance.

In earlier work,[3] we showed that primary particles of the 2D conductor $LiCoO_2$, with high aspect ratios, could be converted into a pseudo-3-D conductor with good performance at high rates, by the preparation of $LiCoO_2$ "balls" with the so-called desert rose morphology. These balls of $LiCoO_2$, and other transition metal doped $LiM_{1-x}Co_xO_2$ (M = Fe, Mn, Ni, etc) samples made by similar methods, are not randomly assembled, but rather are formed by $LiMO_2$ plates that grow out of other plates, with a characteristic angle of ~71° between the connected plates or twins (see Figure 1). Not directly attempting to improve the electrochemical performance of $LiCoO_2$, but as part of a fundamental study initiated to explore the mechanistic and structural origins of this geometric relationship, we now show that with appropriate synthetic conditions, we can control the growth of the plates to prepare an unusual isotropic, concaved cuboctahedron-shaped form of $LiCoO_2$. Hydrothermal methods were used in this study, instead of the low temperature molten fluxes used earlier consisting of LiOH, CsOH, and KOH.[3] The hydrothermal synthesis approach allows for more tunable experimental parameters, (e.g., type and ratio of the starting materials), which are sometimes limited by the melting point

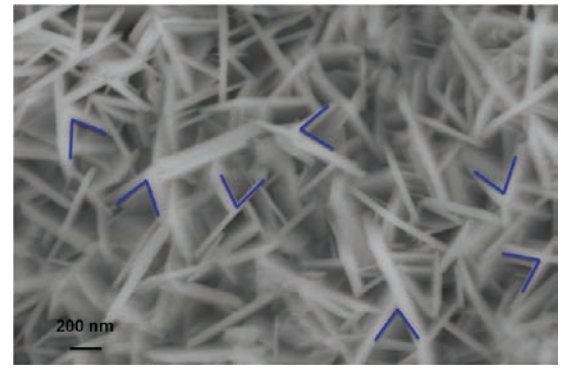

Figure 1. SEM image of the surface of the "desert rose" $LiCoO_2$ balls prepared in our earlier study.[3] Most of the thin rods/plates penetrate or are connected to each other with a characteristic angle of about 71°, as illustrated by the red lines in the figure.

[†] Department of Chemistry, Stony Brook University.
[‡] Brookhaven National Laboratory.
[§] Department of Chemistry, Cambridge University.

(1) Islam, M. S.; Driscoll, D. J.; Fisher, C. A. J.; Slater, P. R. *Chem. Mater.* **2005**, *17*, 5085–5092.
(2) Nishimura, S.; Kobayashi, G.; Ohoyama, K.; Kanno, R.; Yashima, M.; Yamada, A. *Nat. Mater.* **2008**, *7*, 707–711.
(3) Chen, H. L.; Grey, C. P. *Adv. Mater.* **2008**, *20*, 2206–2211.

 10.1021/ja104852q

or solubility in molten flux systems. We first report the synthesis and characterization of a first batch of cuboctahedrons (sample A) and we then describe a detailed investigation of the mechanisms by which they form. An optimized synthesis protocol is devised based on this mechanistic study, leading to the synthesis of a second sample (sample B) with an almost 100% yield of the cuboctahedron morphology.

Experimental Section

Synthesis. Two synthetic procedures were used in this work to prepare the concaved cuboctahedron morphology. In the first procedure (sample A), 0.58 g (2 mmol) $Co(NO_3)_2$ (Sigma-Aldrich, 98%) was dissolved in 5 mL of distilled water to form a clear reddish solution. Seven grams of KOH (Sigma-Aldrich, >85%) and 1 g of LiOH (Sigma-Aldrich, 99%) were dissolved in 10 mL of distilled water. The $Co(NO_3)_2$ solution was then added slowly to the hydroxide solution while stirring. The resulting solution was transferred to a Teflon-lined hydrothermal bomb and was heated statically in an oven at 200 °C for 24 to 48 h. After the bomb was cooled down to room temperature, the product was washed with distilled water and centrifuged several times. Some of the samples were washed with 0.1 M hydrochloric acid to remove the $Co(OH)_2$. The final washed products were dried overnight in an oven at 80 °C.

Higher yields of the concaved cuboctahedron morphology were observed by using a second procedure, in which nanoparticles of CoO or $Co(OH)_2$ with an equivalent amount of Co (2 mmol) were used as the Co source instead of cobalt nitrate (Sample B). The nanoparticles of CoO were prepared by dehydration of commercial $Co(OH)_2$ (Sigma-Aldrich) in a tube furnace under Ar atmosphere at 250 °C for one hour. Nanoparticles of $Co(OH)_2$ (with average particle size of 20 nm) were prepared by a precipitation method: 0.1 M $Co(NO_3)_2$ solution was added slowly into 0.1 M LiOH (Co: Li ratio = 1:2) solution while stirring. The precipitation product was washed with distilled water and dried at 60 °C overnight. An optimal ratio to obtain the highest yield of concaved cuboctahedrons was determined to be LiOH: KOH: H_2O: CoO (or $Co(OH)_2$) 1 g: 3 g: 3 mL: 150 mg (CoO) or 186 mg ($Co(OH)_2$), although increasing the KOH concentration to 7 g (keeping all other reagent concentrations constant) did not alter the yield significantly. The hydrothermal reaction was performed at 200 °C for 24−48 h, to complete the oxidation to Co^{3+} and minimize the impurities, e.g. Co_3O_4. The products were filtered and then washed with distilled water and dried at 70 °C overnight.

Characterization. Powder X-ray diffraction patterns were collected either on a Rigaku MiniFlex diffractometer or at beamline X16C at Brookhaven National Laboratory. The SEM images were taken by using a LEO-1550 field emission scanning electron microscope. JEM-3000F and JEM-2100F high-resolution transmission electron microscopes were used to obtain HRTEM images and single crystal select area electron diffraction (SAED) patterns. The simulations of SAED patterns and HRTEM were carried out using the programs developed in BNL based on the Bloch wave and multislice methods, respectively.

^{7}Li magic-angle-spinning (MAS) NMR spectroscopy was performed on some cuboctahedron $LiCoO_2$ samples and charged "desert rose" $LiCoO_2$ samples (as references) with a 1.8 mm probe on a CMX-200 spectrometer using a magnetic field strength of 4.7 T. A spinning speed of 30 kHz and a rotor-synchronized spin−echo sequence ($\pi/2$-τ−π-τ-acq) were used to acquire the spectra. The ^{7}Li spectra were collected at an operating frequency of 77.10 MHz with $\pi/2$ pulses of 2.5 μs and a delay time of 0.5 s. The spectra were referenced to 1 M ^{7}LiCl in H_2O at 0 ppm.

Electrochemistry. The as-prepared $LiCoO_2$ sample was mixed with poly vinylidene fluoride binder and acetylene black (6:1:3 wt %) in *N*-methyl pyrrolidone (NMP) to make a thick slurry. The slurry was deposited on an aluminum foil by using a doctor-blade method and dried at 80 °C overnight. Coin cells (CR2032, Hohsen Corp.) were assembled in an argon-filled glovebox. Each cell contains typically about 6−8 mg of active material, separated from the Li foil anode by a piece of Celgard separator (Celgard, Inc., U.S.A.). A 1 M solution of $LiPF_6$ in ethylene carbonate/dimethyl carbonate (1:1) was used as the electrolyte. Electrochemical experiments were carried out on a battery cycler (Arbin Instruments, College Station, TX) in galvanostatic mode at various rates.

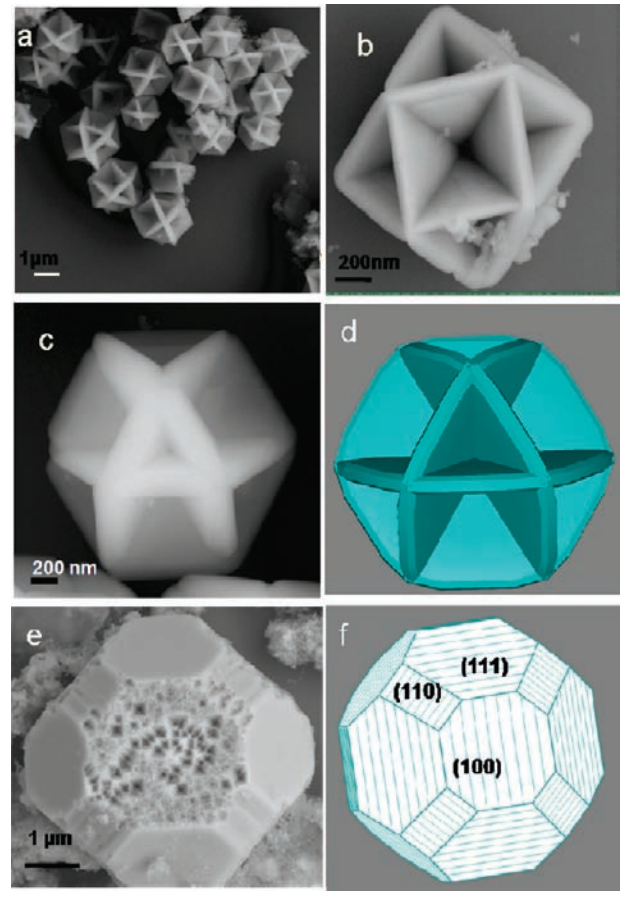

Figure 2. SEM images of (a) concaved cuboctahedron Li_xCoO_2 particles; (b) "[100] " and (c) "[111]" views of a single particle; (d) Schematic drawing of the particle; (e) another morphology obtained in the same sample batch; and (f) schematic of the truncated cube shown in (e) showing the exposed (100), (111), and (110) faces.

Results and Discussion

Synthesis and Characterization of the Cuboctahedron Particles: Sample A. Hydrothermal syntheses of $LiCoO_2$ were performed initially by using starting material combinations similar to those employed in our previous molten flux method (e.g., $Co(NO_3)_2$ (0.58 g), LiOH (1 g), and KOH (7 g), H_2O (15 mL), corresponding to molar ratios of 1:21:53: 417, respectively),[3] except that CsOH was omitted in this study and water was employed as the solvent. Surprisingly, the final product of a 24 h reaction at 200 °C contained regular, uniform and extremely unusual concaved cuboctahedron-shaped crystals, as seen by SEM (Figure 2 a−c) as a minor morphology. Figure 2d shows a computer-generated drawing of the particle, based on the SEM images of the particles viewed from different directions (Figure 2b−c). Each cuboctahedron particle consists of four equivalent hexagonal plates, with angles between two of these plates of 70.5°, so as to maintain overall cubic symmetry. The angles between the plates are the same as those observed in our earlier syntheses of "desert rose" $LiCoO_2$ (Figure

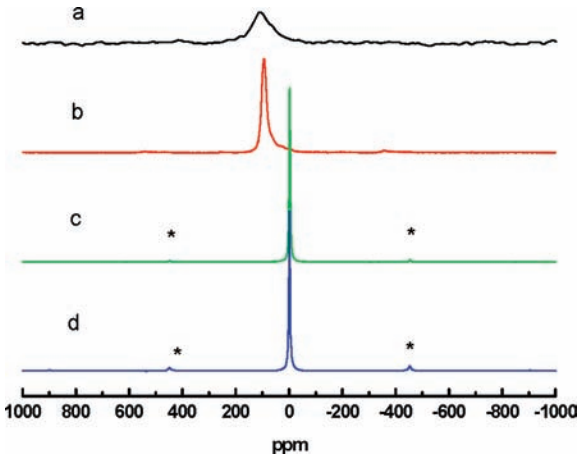

Figure 3. ^{7}Li MAS NMR spectra of (a) the first synthesis (sample A), (b) 90% charged stoichiometric (desert-rose) $LiCoO_2$, (c) pristine desert rose $LiCoO_2$, and (d) the second synthesis (sample B; stoichiometric, cuboctahedron $LiCoO_2$). The spinning side bands are indicated by asterisks in c and d.

1). To the best of our knowledge, this cuboctahedron morphology has only been reported once before, for CuS by Wu et al.,[4] but no detailed growth mechanism was proposed.[4] Our crystals are, however, much more uniform than the CuS particles and always comprise 4 hexagonal plates, while the CuS particles sometimes contained only 2 or 3 plates. Apart from the geometrical simplicity and the aesthetic qualities of these crystals, a number of scientific questions are raised, which include the structure of the material and how and why it forms.

The X-ray diffraction (XRD) pattern of the product shows the presence of a mixture of $Co(OH)_2$, CoO, and $LiCoO_2$, $Co(OH)_2$ being formed from the reaction of $Co(NO_3)_2$ and OH^-, and CoO from the decomposition of the unstable $Co(OH)_2$ phase.[5] After quickly washing the product by using 0.1 M HCl to dissolve the $Co(OH)_2$ phase, only CoO and $LiCoO_2$ are seen by XRD, while the cuboctahedrons are still observed by SEM. This indicates that the cuboctahedron are either CoO or $LiCoO_2$. The acid wash was only performed on one batch solely to exclude the possibility that the concaved octahedrons were due to the acid-soluble phase, $Co(OH)_2$. Rietveld refinement was applied to the XRD pattern of the mixture (see Figure S1b in the Supporting Information, SI). The *c* parameter of the $LiCoO_2$ phase extracted from the refinement is 14.21 Å, slightly larger than the usual value of bulk $LiCoO_2$, which is around 14.06 Å.[6] This suggests that this $LiCoO_2$ phase may not be stoichiometric.

^{7}Li MAS NMR spectroscopy was performed to explore the Li nonstoichiometry of the lithiated phase, since the method is extremely sensitive to small deviations in the stoichiometry of the $LiCoO_2$ phase.[7] A broad resonance at 100 ppm is observed of the sample (Figure 3a), rather than the single shift at 0 ppm expected for a stoichiometric, diamagnetic $LiCoO_2$ sample.[7] The spectrum of the sample of the "desert-rose" form of $LiCoO_2$ charged to 90% is shown for comparison (Figure 3b). This similarly contains a resonance at ~100 ppm, which is consistent with other charged stoichiometric samples which resonate at 60−100 ppm for Li_xCoO_2, $x < 0.75$.[7] The shift seen in these latter samples is caused by the Knight shift, which indicates that the sample is metallic. Although we have not analyzed the origin of the shifts of the cuboctahedron sample in any detail, the NMR results reveals that the first batch $LiCoO_2$ is not stoichiometric. The electrochemical capacity of this sample is also low, when it is used as an electrode material in a lithium-ion battery (~30−50 mAh/g between 2−4.8 V), again indicating that this $LiCoO_2$ phase is not stoichiometric.

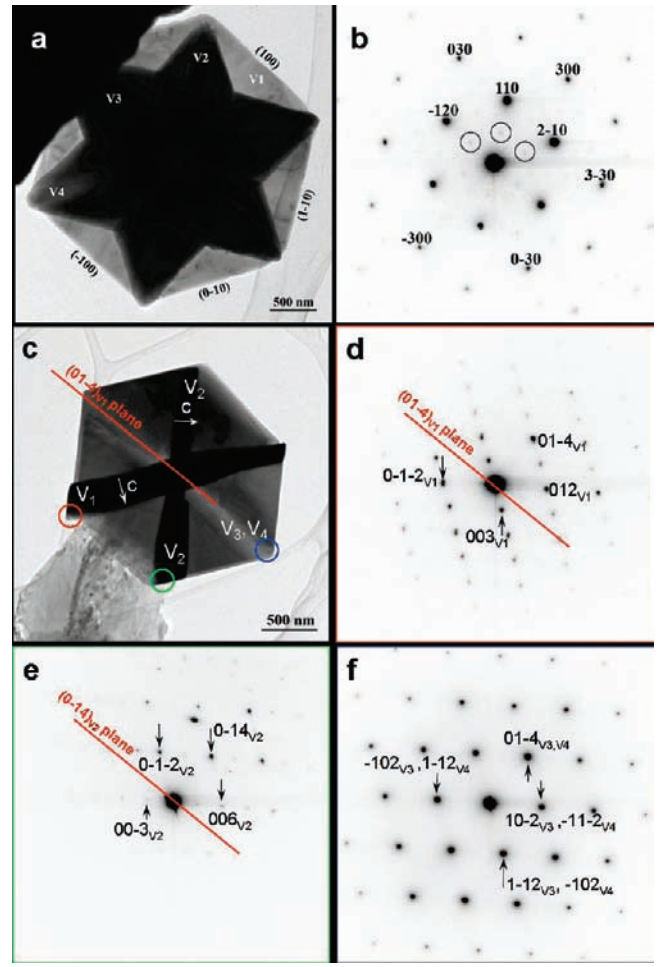

Figure 4. Morphology of a concaved cuboctahedron (a) viewed along the normal of the V1 plate. (b) Selected-area diffraction (SAED) pattern of V1. (c) View along the [−100]V1 or the equivalent [100] V2, or [241]V3, or [−2−4−1]V4 directions. (d−f) SAED patterns of the different twin variants of Li_xCoO_2: (d) [−100]V1 (from red circled area); (e)[100]V2 (from green circled area); (f)[241]V3 and [−2−4−1]V4 (blue circled area).

Twinned Nanocrystals: Transmission Electron Microscopy Study of Sample A. Structure. Although it is difficult to determine which of the phases seen by powder XRD corresponds to the cuboctahedrons in the mixture, and the size of the cuboctahedrons is too small for single crystal XRD studies, electron diffraction on a single particle under TEM provides an effective method with which to investigate their structure. A transmission electron microscopy (TEM) image of a concaved cuboctahedron viewed along the normal direction of one hexagonal plate (labeled as V1) is shown in Figure 4a. The selected-area electron diffraction (SAED) pattern taken from the V1 plate is shown in Figure 4b. This pattern contains bright spots that can be indexed with the $[001]_H$ pattern of Li_xCoO_2

(4) Wu, C. Y.; Yu, S. H.; Antonietti, M. *Chem. Mater.* **2006**, *18*, 3599–3601.
(5) Lide, D. R. *CRC Handbook of Chemistry and Physics*; Section 4, 79th Edition; CRC press: Florida, USA.
(6) Okubo, M.; Hosono, E.; Kim, J.; Enomoto, M.; Kojima, N.; Kudo, T.; Zhou, H. S.; Honma, I. *J. Am. Chem. Soc.* **2007**, *129*, 7444–7452.
(7) Menetrier, M.; Saadoune, I.; Levasseur, S.; Delmas, C. *J. Mater. Chem.* **1999**, *9*, 1135–1140.

(where the subscript H denotes the index based on the hexagonal lattice of $LiCoO_2$). The spots are not consistent with either CoO or Co_3O_4: the lattice parameters of Li_xCoO_2 and CoO are sufficiently different to allow these two phases to be resolved, while those due to Co_3O_4 and $LiCoO_2$ can be distinguished based on differences in the extinction conditions. The normal of the hexagonal plate is $[001]_H$, while its edges are indexed as $(100)_H$, $(010)_H$ and $(1\bar{1}0)_H$. The very weak spots in Figure 4b, indicated by the black circles, suggest the presence of a 2a × 2a $LiCoO_2$ superstructure. This superstructure is tentatively ascribed to either long-range ordering due to partial Co occupancy on the Li site, and/or proton or vacancies on the Li site, indicating some nonstoichiometry of the $LiCoO_2$ particles, consistent with the NMR results for the sample.

Twinning. Nanoparticles with unusual, highly symmetric morphologies have been reported for various functional materials, including noble metals catalysts[8,9] and semiconductors.[10,11] However, in these cases, the symmetry of the particle is consistent with the symmetry of the lattice of the material, different morphologies simply resulting from different crystal truncations and preferred growth directions of the particles. By contrast, $LiCoO_2$, either the stoichiometric or nonstoichiometric versions, adopts a layered, hexagonal lattice and yet the concaved cuboctahedrons show overall cubic symmetry. The question that must now be answered is: how and why do the four hexagonal plates grow together to form an isometric crystal? In principle, twinning represents one way to break the intrinsic symmetry of a crystal. However, it usually results in additional sets of reflections in the diffraction patterns of the twinned crystal, due to a loss of symmetry of the overall particle; this is not the case for the cuboctahedrons (see Figure 4). Given that the lattice of $LiCoO_2$ can be described by a rhombohedral unit cell with $\alpha \approx 89.88°$, i.e., the deviation from the cubic unit cell is small, certain classes of twin variants may be present in which the splitting or doubling of the reflections may not be distinguishable in the SAED pattern due to the limited set of reciprocal vectors that we are probing. However, the existence of the twins can be verified based on the different extinctions between the SAED patterns along the real 3-fold and the pseudo-3-fold axes (Figure 4c−f). The SAED patterns shown in Figure 4d−f are taken from different areas indicated by the circles and arrows in Figure 4c, without changing the tilt angle of the crystal. Patterns d and e can be indexed as $LiCoO_2$ diffraction patterns along the [100] zone axis for plate V1 and [−100] for the second plate V2, respectively, and the c axes of V1 and V2 twin variants can therefore be determined, as labeled in the figure (see Supporting Information for more details). The angle between the *c* axes of V1 and V2, which is also the angle between the *c** axes of their reciprocal lattice, is 70.5°, consistent with the angle between the {111} planes expected for a cubic system. The V1 and V2 twins are, thus, related by a reflection on the (0−14) plane. The reflections for the V3 and V4 plates are superimposed when viewed down the [241] axes of V3 (Figure 4f). On the basis of this analysis, it is clear that the concaved cuboctahedron consists of four hexagonal plates, with each plate being a twin variant. The plate normal is the *c* axis (the 3-fold axis) of the variant (i.e., the Li_xCoO_2 plate).

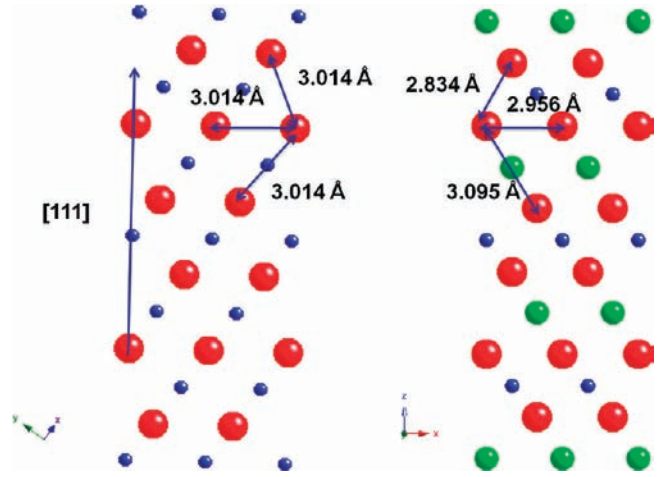

Figure 5. (a) Projection of the CoO lattice along the [10−1] direction, showing the stacking of atoms along [111] direction; (b) Projection of $LiCoO_2$ lattice along the *b* direction, showing the stacking of atoms along [001] direction. Oxygen, cobalt, and lithium atoms are plotted as red, blue, and green balls, respectively.

The Growth Mechanism. In order to determine how and why the cuboctahedrons grow to form this morphology, we carefully examined the first synthesis batch for any clues in the form of other phases and particles that are present in this sample. Large crystals were also seen in this batch before and after washing, which consist of regular polygons with small pit marks on select faces. Figure 2e shows a cropped SEM image of one of these crystals, which are geometrically derived by truncating the edges and corners of a cube, exposing the {100}, {111}, and {110} faces. This is illustrated in Figure 2f, which shows a model of the truncated cube. Although much larger in size, these cubic crystals are fewer in number in the product mixture (see Figure S1c in the SI for a lower magnification SEM image of the same mixture), than the noticeably smaller particles of the other components. The larger particles are ascribed to the cubic material CoO (space group $Fm\bar{3}m$, $a = 4.26$ Å), since the reflections of CoO in the XRD patterns are very sharp and intense (see Figure S1b in the SI). The crystals show pronounced selective pitting of their {100} faces to expose the {111} planes, no pits being observed on the {111} faces. One explanation for this selectivity is that the {111} faces are charge polarized, so that they are more easily stabilized by electrical double layers, making it more difficult to extract an ion from the surface; in contrast, the {100} faces are charge neutral, and the Co^{2+} and O^{2-} ions can be extracted more readily.[12] Pitting in highly basic solutions occurs in many materials, and in more exceptional cases, as seen for example in PbS cubes under select conditions, can result in concave, regularly shaped (in this case pyramidal) pits which alter the morphology of the whole particle.[13] Solely on the basis of the geometry of the two objects, a concaved cuboctahedron can be formed directly from a cube, via pitting to maximize the surface area of the {111} faces.

The lattices of CoO and $LiCoO_2$ are similar, the rhombohedral distortion of the unit cell of $LiCoO_2$, with $\alpha \approx 89.88°$, being extremely small. Figure 5a shows the stacking of the CoO atoms along the [111] direction and b shows the stacking of atoms of $LiCoO_2$ along [001] direction. The stacking of the two lattices

(8) Sun, Y. G.; Xia, Y. N. *Science* **2002**, *298*, 2176–2179.
(9) Tian, N.; Zhou, Z. Y.; Sun, S. G.; Ding, Y.; Wang, Z. L. *Science* **2007**, *316*, 732–735.
(10) Manna, L.; Milliron, D. J.; Meisel, A.; Scher, E. C.; Alivisatos, A. P. *Nat. Mater.* **2003**, *2*, 382–385.
(11) Manna, L.; Scher, E. C.; Alivisatos, A. P. *J. Am. Chem. Soc.* **2000**, *122*, 12700–12706.
(12) Vayssieres, L.; Keis, K.; Hagfeldt, A.; Lindquist, S. E. *Chem. Mater.* **2001**, *13*, 4395–4398.
(13) Hou, Y.; Kondoh, H.; Ohta, T. *Cryst. Growth Des.* **2009**, *9* (7), 3319−3123.

are very similar in terms of the closest O−O distances within the layer and between layers (in particular, the O−O distances defining the Li^+ and Co^{2+} octahedra and thus layers are similar) and only differ in the nature and stacking of the metal layers. The $LiCoO_2$ lattice can be derived from CoO by replacing every other (111) layer of Co by Li so that the 3-fold symmetry along 3 out of 4 ⟨111⟩ directions is lost. Thus, the $LiCoO_2$ cuboctahedrons can, at least from a *crystallographic* point of view, be derived by a combination of CoO lithiation and selective pitting. The lithiation of CoO can in principle occur via Li^+/Co^{2+} ion exchange of alternate layers, a process that must be accompanied by the oxidation of remaining Co^{2+} in the lattice to Co^{3+} for charge balance, the oxidation of a Co^{2+} ion nearby an inserted Li^+ ion being favored on the basis of electrostatics. The basic conditions used here should increase the stability of Co(III) over Co(II), driving this process and hindering dissolution of the ion-exchanged Co^{3+} phase.[3] Li^+/Co^{2+} exchange is likely to be rapid at, or close to the surface, of the crystal, but is unlikely to be fast for the whole crystal. Thus, the Li layers at the center of the crystal may not be fully lithiated. Furthermore, this mechanism will be less effective for large micrometer-sized particles. We note that there is precedence for rapid ion-exchange reactions in nanoparticles in materials where the bulk reactions are slow.[14,15] A number of phenomena are thought to be responsible for this phenomenon, including (i) the strong particle-size dependence for ion-exchange involving diffusion controlled reactions, (ii) the fact that the reaction fronts in ion-exchange reactions can be similar to the size of the nanomaterial, so that a sharp interface between the non and lithiated phases (in this system) are not observed, and (iii) the increased flexibility of nanosystems to accommodate expansions/contractions of the layers.

Since the original proposed crystal template (CoO) is cubic, $LiCoO_2$ has an equal probability of being generated with its unique 3-fold axis (the *c* axis in a hexagonal lattice) along the [111], [11−1], [1−11], or [−111] axes of the parent phase (CoO). Thus, four twin variants can simultaneously grow from the same parent CoO crystal to generate a 4-fold twinned crystal that, despite the symmetry of the phase that grows, can maintain overall cubic symmetry. A more rigorous analysis of the $LiCoO_2$ twins, by using the space group theory on domain formation during a disorder−order structural transformation[16] (as described in detail in the SI), is consistent with this suggestion: $LiCoO_2$ adopts the space group $R\bar{3}m$, which is a subgroup of the space group adopted by CoO ($Fm\bar{3}m$). On the basis of the orders of the two groups, it is straightforward to show that there will be four twin variants with orientations between them consistent with the observed cuboactahedrons.

Finally, it is important to note that while in principle, ion-exchange (and oxidation) of both $Co(OH)_2$ and CoO are possible, both phases being present in the reaction mixture (Figure S1a,b in the SI), it is not clear how the former phase can act to template the symmetric cuboctahedron. Consistent with this, in our earlier synthesis of "desert-rose" $LiCoO_2$, where $LiCoO_2$ grew from $Co(OH)_2$ template crystals, no symmetric cuboctahedrons were observed.[3] CoOOH is excluded because we never saw any evidence for this phase in any of the XRD patterns extracted from the hydrothermal mixture.

Synthesis of the Stoichiometric $LiCoO_2$ Cuboctahedrons: Sample B. The role of CoO in templating the growth of $LiCoO_2$ has not, to our knowledge, been reported before. The usual precursors used in the solid state reactions to form $LiCoO_2$ are either CoOOH[17] or Co_3O_4,[18] where the Co is already fully or partially oxidized to Co(III). As the Li_xCoO_2 cuboctahedrons were not the major phase/morphology in our first sample batch, we strove to provide additional support for the formation mechanism by improving the yield of this morphology, using the proposed growth mechanism as a guide with which to optimize the reaction conditions. To this end, when commercial (∼5 μm size) CoO was used as the Co source as a replacement for $Co(NO_3)_2$ in the hydrothermal synthesis, very few cuboctahedrons and more pitted large crystals were seen in the products, indicating that the size of the parent crystal is crucial in controlling the morphologies formed in this reaction. To reduce the size of parent crystal, ∼50 nm sized particles of CoO, prepared by decomposition of commercial $Co(OH)_2$, were used as the Co source. This led, after 48 h, to the formation of $LiCoO_2$ and Co_3O_4 as the major and minor phases, respectively. Many more cuboctahedrons were seen in this sample. This is consistent with the suggestion that the Li^+-Co^{2+} ion-exchange/Co^{2+} oxidation reaction is key to the formation of the cuboctahedron, since this reaction should be favored for nanoparticles. The appearance of Co_3O_4 is ascribed to a second oxidation process that competes with the lithiation-oxidation reaction under these conditions.

Experiments were performed using Co_3O_4 particles as the Co source, to explore the role of Co_3O_4 (see SI for more details), which revealed that although the larger Co_3O_4 particles were stable under the basic hydrothermal reaction conditions used here, nanoparticles of Co_3O_4 converted to $LiCoO_2$. However, no concaved cuboctahedron particles were ever observed, even after long reaction times, indicating that Co_3O_4 does not appear to serve as a template crystal for this morphology. Again this suggests that it is CoO, and not Co_3O_4, that is the template of the cuboctahedrons.

Both increased pH and Li^+ concentration should favor Li ion-exchange (reaction 1) according to the following reactions:

$$4CoO + 1/2O_2 + 2Li^+ + 6OH^- + H_2O \rightarrow 2LiCoO_2 + 2Co(OH)_4^{2-} \quad (1)$$

$$4CoO + 1/2O_2 + 2OH^- + H_2O \rightarrow Co_3O_4 + Co(OH)_4^{2-} \quad (2)$$

or

$$3CoO + 1/2O_2 \rightarrow Co_3O_4 \quad (3)$$

the latter reaction occurring without Co^{2+} dissolution. We note that reactions (1) and (2) will be limited by the solubility of $Co(OH)_4^{2-}$. Thus further reaction must proceed by the precipitation $Co(OH)_4^{2-}$ as CoO, $Co(OH)_2$, or directly as $LiCoO_2$ (see later). It is important to note that these reactions represent a simplified form of the many reactions and equilibria occurring in this system; for a discussion of the separate reactions please see the SI. However, consistent with these reactions, when the LiOH concentration was reduced, less $LiCoO_2$ and more Co_3O_4

(14) Son, D. H.; Hughes, S. M.; Yin, Y. D.; Alivisatos, A. P. *Science* **2004**, *306*, 1009–1012.
(15) Dloczik, L.; Konenkamp, R. *Nano Lett.* **2003**, *3*, 651–653.
(16) Wu, L. J.; Zhu, Y. M. *Philos. Mag. A* **1997**, *76*, 481–492.
(17) Pralong, V.; Delahaye-Vidal, A.; Beaudoin, B.; Gerand, B.; Tarascon, J. M. *J. Mater. Chem.* **1999**, *9*, 955–960.
(18) Shao-Horn, Y.; Hackney, S. A.; Johnson, C. S.; Kahaian, A. J.; Thackeray, M. M. *J. Solid State Chem.* **1998**, *140*, 116–127.

was formed and fewer or no cuboctahedrons were seen. In contrast, on reducing the amount of water used in the reactions, while keeping all of the other reagents constant, more cuboctahedrons and less Co_3O_4 were seen. This was ascribed to the increase in pH and Li^+ concentration. The additional empty space left in the hydrothermal vessel will increase the amount of air/O_2, but this additional O_2 is not sufficient to prevent cuboctahedron formation. On completely removing water from the starting materials, for example by performing a molten salt reaction in the sealed hydrothermal bomb, no concaved cuboctahedrons are seen, presumably because the $Co(OH)_4^{2-}$ solubility is reduced further.

An analysis of the results from all our synthetic attempts described above suggested that nano-$Co(OH)_2$ might be a better starting material than CoO for this reaction. This hypothesis was based on the observation that under hydrothermal heating at 200 °C, nano-$Co(OH)_2$ will quickly decompose to form nanosized CoO particles, and the hypothesis that, under optimized conditions, the ion exchange and oxidation reactions should occur before the newly formed CoO nanoparticles aggregate and grow larger. To test this hypothesis, laboratory-synthesized ~20 nm $Co(OH)_2$ particles were used, and much higher yields of the cuboctahedrons were observed. Using this nano-$Co(OH)_2$ along with an optimized amount of water of 3 mL (e.g., 1 g of LiOH, 3 mL of H_2O and 3 g of KOH with 186 mg $Co(OH)_2$ as starting materials), led to essentially phase-pure $LiCoO_2$, with the uniform cuboctahedrons representing the overwhelming morphology (Figure 6a,b). The optimum water content was found by reducing the water concentration systematically keeping all other reagent concentrations (used to prepare sample A) constant and monitoring the cuboctahedron yield. Reducing the KOH:LiOH concentration from 7 to 3 did not alter the yield noticeably. CoO still presumably acts as the template crystal, but it now has an even smaller particle size and higher reactivity than the 50 nm CoO precursor also tested (see earlier), since it is formed *in situ* by decomposition of the 20 nm $Co(OH)_2$. (See SI for further evidence for the formation of precursor CoO crystals in this reaction). This also helps explains the coexistence of the giant pitted CoO crystal and the cuboctahedrons in the first batch (sample A); since the $Co(OH)_2$ phase formed from the reaction of $Co(NO_3)_2$ and OH^- has a broad size distribution this will also result in a broad size distribution of CoO crystals formed from $Co(OH)_2$ decomposition. The smaller CoO crystals are then ion-exchanged and oxidized forming the concave $Li_xCo_{1-x}O$ crystals, which grow to become the micrometer size cuboctahedron $LiCoO_2$, while the large CoO crystals keep growing and are only heavily pitted, but cannot be completely converted to the fully concaved and lithiated structure.

Characterization of the Stoichiometric Cuboctahedrons. The high-yield cuboctahedron sample, based on a range of analyses, has a composition that is extremely close to stoichiometric $LiCoO_2$ and only a trace amount of Co_3O_4 is detected in the XRD pattern (see Figure 7). Cell parameters of $a = b = 2.814(6)$, $c = 14.046(5)$ Å for $LiCoO_2$ are extracted via Rietveld refinement (with wRp = 8.05%.), which are within the ranges expected for stoichiometric micrometric $LiCoO_2$[6] and direct coupled plasma (DCP) analysis gives a Li:Co ratio of 1.05(±0.05):1. The ^{7}Li MAS NMR spectrum of this sample is shown in Figure 3d. It is very similar to the spectrum of stoichiometric $LiCoO_2$ (for example the "desert rose" form shown in Figure 3c): the spectrum is dominated by a signal at 0 ppm, which is due to the diamagnetic environments of Li

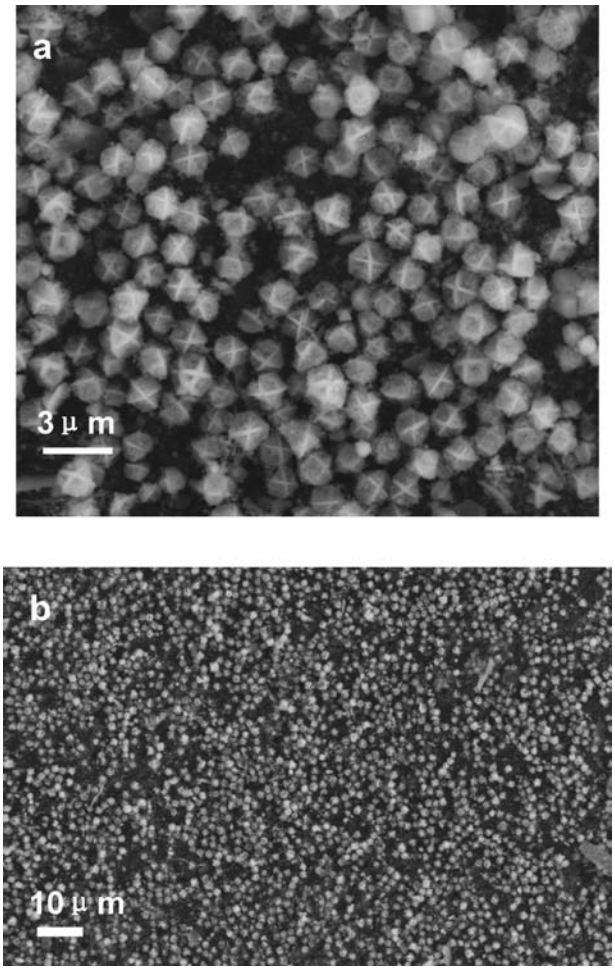

Figure 6. (a) High magnification and (b) larger scale SEM image of phase-pure $LiCoO_2$ with the cuboctahedron morphology.

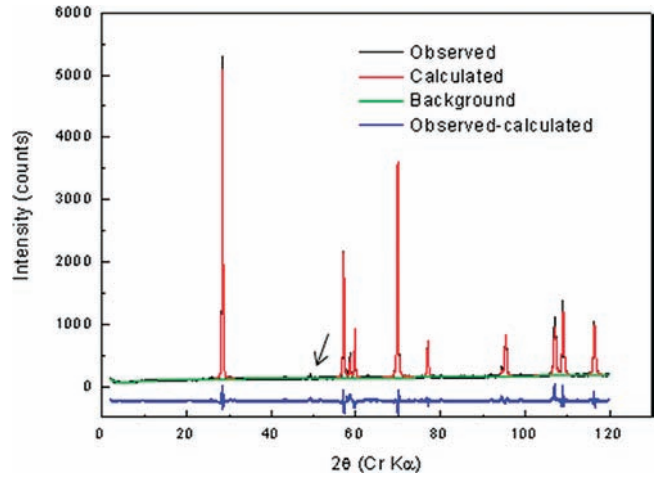

Figure 7. The XRD pattern and Rietveld refinement of the high yield cuboctahedron $LiCoO_2$. The black arrow indicates the characteristic reflection of the Co_3O_4 impurity.

surrounded by Co^{3+} (d^6), and none of the resonances characteristic of nonstoichiometry are observed (Figure 3d). Consistent with this, no superstructure reflections were detected in the SAED pattern of this sample (see Figure 8d), in contrast to the SAED patterns obtained from the first batch (Figure 8b). Although this concaved shape is not ideal for creating a high density compact cathode with high volumetric power density,

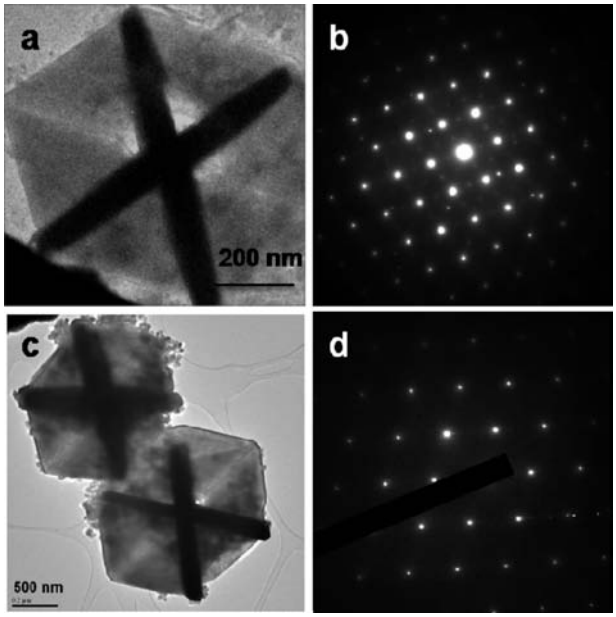

Figure 8. TEM studies of the cuboctahedra: (a) Morphology of nonstoichiometric Li_xCoO_2 concaved cuboctahedra (route A), and (c) stoichiometric $LiCoO_2$ concaved cuboctahedra (route B). The scale bars in (a) and (c) are 200 and 500 nm, respectively. Parts (b) and (d) are SAED patterns of the particles shown in (a) and (c) along the same ($[214]_H$) zone axes.

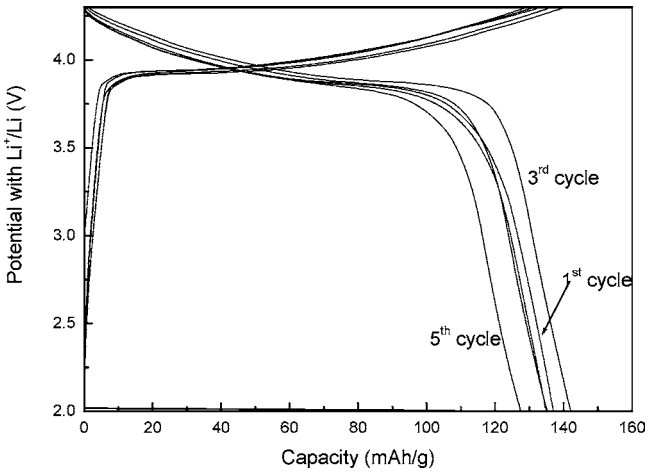

Figure 9. Charge and discharge curves for the first 5 cycles for high-yield cuboctahedron $LiCoO_2$. The cycling window is 2−4.3 V. A current density of 200 mA/g, corresponding to a rate of 1.5C was used.

the $LiCoO_2$ form yields a moderate capacity of 142 mAh/g at a rate of 1.5 C, as shown in Figure 9. At lower rates, e.g., C/15, the capacity of this material is about 135 mAh/g between 2.5 and 4.3 V, being similar to that of commercial $LiCoO_2$.[19]

Summary and More Detailed Analysis of the Growth Mechanism

The proposed mechanism for the growth of the cuboctahedrons can now be summarized as follows: a parent (template) nanocrystal of CoO pits from all 6 [100] directions. At the same time, due to the high Li^+ concentration, Li^+ starts to insert into the CoO lattice by exchanging with Co^{2+} in the {111} planes. Correspondingly, upon one Li^+ insertion/exchange, one Co in the neighboring layer is oxidized to Co(III) to maintain charge neutrality, via a mechanism that we refer to as a simultaneous "oxidation-ion-exchange" reaction. Since Co(III) is much more stable and Co(II) is less soluble in the basic solution, the Co(III) layer is stabilized by this Li insertion. The Li ions continue to exchange with Co(II) until they approach the center of the mother CoO nanoparticle, alternating Li and Co^{3+} layers being favored by the same driving forces that favor layered $LiCoO_2$.[20] Dissolution will also occur on other faces, such as the {110} and {111} faces, always leaving behind stable {111} faces. At the same time, Co(II) in solution (largely $Co(OH)_4^{2-}$) will also be oxidized to Co(III) and will reprecipitate together with Li^+ and oxide ions on the surface of the newly formed $LiCoO_2$-like domains, $LiCoO_2$ growing along the $[001]_H$, $[010]_H$, and $[110]_H$ directions, as observed in our previous study.[3] This also gives rise to the characteristic angles between the $LiCoO_2$ plates seen in both the desert rose (Figure 1) and cuboctahedron morphology. Note that this precipitation must occur so as to consume the $Co(OH)_4^{2-}$ produced by ion-exchange mechanism (reaction 1). Finally, via simultaneous pitting and growth, the parent CoO crystal gradually adopts a concaved cuboctahedron shape, as illustrated in Figure 10a.

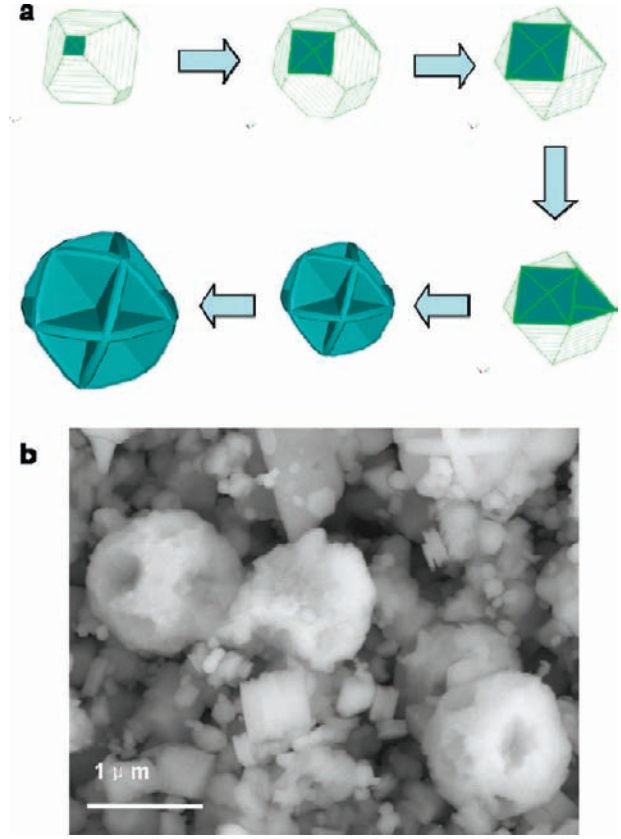

Figure 10. (a) Growth mechanism of the concaved cuboctahedron. Areas shown in dark represent the leached planes. For clarity, only one set of leached planes is shown for each stage and the size of the parent crystal and the final twin crystal is not proportionally scaled: in the experiments, the parent crystals are only ∼20−50 nm and the final twin crystals are about 1 μm. (b) Example of an "intermediate" morphology.

The real growth process will be more complicated than the simplified case shown in Figure 10a. First, irregular intermediate morphologies are expected before the particles finally grow into

(19) Ohzuku, T.; Ueda, A.; Nagayama, M. *J. Electrochem. Soc.* **1993**, *140*, 1862–1870.

(20) Wu, E. J.; Tepesch, P. D.; Ceder, G. *Philos. Mag. B* **1998**, *77*, 1039–1047.

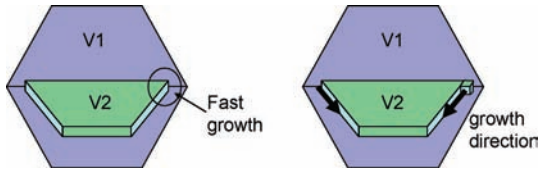

Figure 11. A schematic showing the fast growth on the edge of the $LiCoO_2$ plates, which results in the equivalent size of the four twin crystals and the perfect overall cubic symmetry.

the regular concaved cuboctahedron shape. An example of this is shown in Figure 10b, where crystals that are heavily leached but have not yet achieved a concaved cuboctahedron shape can be seen. This sample was synthesized by using micrometer-sized CoO particles as the cobalt source, the particles presumably being too large to be completely converted to cuboctahedrons. Second, the parent CoO template crystals do not have to adopt regular shapes as shown in Figure 10a, the CoO formed by decomposition of an anisotropic material such as $Co(OH)_2$, for example, still leading to a perfectly symmetric cubocahedron. This can be explained by the preferred fast growth of $LiCoO_2$ along [100], [010] and [110] directions and Oswald ripening: Although the parent CoO crystal can be irregular in shape, once it forms the prototype of the cuboctahedron, e.g., once it has all four $LiCoO_2$ twin variants, no matter how different they are in size and shape, the four variants will grow along their own [100], [010], and [110] directions. If one of the 4 twin variant (plates) of $LiCoO_2$ cuboctahedron, e.g., V2, as schematically drawn in Figure 11, is smaller than any of the other plate(s), e.g., V1 (for clarity, the other two plates are not shown), then at the region where the edge of the V2 plate contacts the V1 plate, as indicated by a black arrow in Figure 11 (left hand side), a concaved shape or v-shape is formed. Addition of ions at this intersection will be faster, as generally seen for growth at steps in crystals, due to the availability of higher coordination number sites on the surface, causing quick growth of a step away from the intersection of the plates. Fast growth of other parts on the edge of V2 will occur as the step moves out, away from the twin boundary, as shown in Figure 11 (right). Meanwhile, growth at the intersection of the two plates will continue, until eventually V2 becomes the same size as V1. This effect applies for any two of the plates. Thus, overall, the higher surface energy areas at the intersections will vanish leading to four plates with exactly the same size, as is consistently seen experimentally.

At least three factors appear to be important in the nucleation of and growth of the cuboctahedrons. First, the ability of the parent crystal, nanoparticulate CoO to undergo ion-exchange and oxidation of the Co^{2+} to form seed nuclei of $LiCoO_2$ on the CoO surface, and leaching of select faces to expose stable surfaces. Co_3O_4, for example, which contains alternating Co^{3+} and Co^{2+} (tetrahedral) and Co^{3+} octahedral layers, does not form an ideal template crystal because Li^+/Co^{3+} exchange (in the Co^{2+}/Co^{3+} layers) is very difficult, requiring Co^{3+} mobility and dissolution. Second, a c/a ratio of $LiCoO_2$ that is close to that of a cubic material, along with the likely ability of this material to accommodate slight variations in stoichiometry of the Li_xCoO_2 phase at the twin boundaries, allows 4 twins with rhombohedral symmetry to grow, with minimal stress at the interconnects of the 4 plates.

Finally, the symmetry of the parent crystal and the phase that grow on it will control the nature of the morphology of the final particle, and the number and types of twins formed. For example, when nanometer sized FeO was used as starting material in a related synthesis, the final product, $LiFeO_2$, which has a tetragonal lattice, shows a very different morphology for the final twinned crystal, but again it is determined by the symmetry relationships between the parent (FeO) and final product (see Figure S5 in the SI). Although the use of seed crystals (of Ag[21] and Pt,[22] for example) to template growth on distinct crystal facets to control morphology has been reported by others, the growth of cuboctahedrons is distinct from these growth mechanisms, since the final morphology is determined by the different symmetry of the template and the final product.

The formation of cuboctahedrons is not limited to $LiCoO_2$ and Fe, Mn and Ni-doped $LiCoO_2$ concaved cuboctahedrons have been observed when using Fe-, Mn-, and Ni-doped CoO/$Co(OH)_2$ as starting materials. The yields are lower, and more careful optimization of the synthesis conditions is required for each specific starting material combination (see Figure S4 in the SI). The cuboctahedrons themselves are not the most ideal morphology for a cathode material and do not lead to a high rate electrode material. One reason for the poor rate performance may be the pinning of the layers at one end of the crystal: this means that the twinned particles may not be able to accommodate the significant changes in the interlayer spacings that occur on cycling. We note, however, that the pinning of the layers should help to prevent the shearing of the oxygen layers that occurs at high voltage.[23−25] We hope that an understanding the formation mechanisms of this kind of twinning and particle assembly will be very helpful for designing future 3-D nanostructures and mesostructures, as exemplified by the "desert rose" $LiCoO_2$ morphology, which does show very good rate performance.

Conclusions

A unique morphology for $LiCoO_2$ comprising of concaved cuboctahedrons has been observed and its formation has been rationalized in terms of an oxidation-ion-exchange and isotropic growth mechanism. Near 100% yield was achieved by optimizing the starting materials and synthesis conditions according to the proposed growth mechanism. The final product ($LiCoO_2$) maintains its own symmetry (rhombohedral) with a twinned assembly governed by the symmetry of the precursor (cubic). The number of twins and their orientations can be determined by an analysis of the space groups adopted by these two morphologies and their supergroup, subgroup relationships. The work not only describes a new topological reaction, but the results also open up new strategies for designing novel morphology of crystals by exploiting the differences in symmetry between the precursor and the products. This suggests new routes for tuning the morphology and symmetry of crystals by systematic crystal engineering. Finally, the ability to grow physically and electronically connected crystals may in the future lead to strategies to improve rate, as shown earlier by the desert rose form of $LiCoO_2$.[3]

Acknowledgment. We thank James Quinn, George Hart, and Dong Su for help with the electron microscopy data collection and

(21) Fan, F. R.; Ding, Y.; Liu, D. Y.; Tian, Z. Q.; Wang, Z. L. *J. Am. Chem. Soc.* **2009**, *131*, 12036–12037.
(22) Habas, S. E.; Lee, H.; Radmilovic, V.; Somorjai, G. A.; Yang, P. *Nat. Mater.* **2007**, *6*, 692–697.
(23) Amatucci, G. G.; Tarascon, J. M.; Klein, L. C. *J. Electrochem. Soc.* **1996**, *143*, 1114–1123.
(24) Van der Ven, A.; Aydinol, M. K.; Ceder, G. *J. Electrochem. Soc.* **1998**, *145*, 2149–2155.
(25) Van der Ven, A.; Aydinol, M. K.; Ceder, G.; Kresse, G.; Hafner, J. *Phys. Rev. B* **1998**, *58*, 2975–2987.

mathematical modeling, Peter Stephens for synchrotron XRD, and Yuanzhi Tang for DCP analysis. This work was supported by the Assistant Secretary for Energy Efficiency and Renewable Energy, Office of FreedomCAR and Vehicle Technologies of the U.S. DOE under Contract No. DE-AC03-76SF00098 via Subcontract No. 6517749 with the Lawrence Berkeley National Laboratory. Research carried out at Brookhaven National Laboratory was supported by the U.S. DOE under Contract No. DE-AC02-98CH10886.

Supporting Information Available: 1. Non-stoichiometric $LiCoO_2$: XRD and refinement for sample A; additional TEM data and relationship between the four twin variants; detailed analysis of the SAED data. 2. Additional discussion and experimental support of the growth mechanism: reactions and equilibria in the system; investigation of the role of Co_3O_4; in situ formation of nano-CoO. 3. Transition metal doped $LiCoO_2$ cuboctahedrons. 4. FeO and $LiFeO_2$ twinned crystals. This material is available free of charge via the Internet at http://pubs.acs.org.

JA104852Q